New Journal of Physics

PAPER

Grüneisen approach for universal scaling of the Brillouin shift in gases

Kun Liang[1] , Jiaqi Xu[1], Yuanqing Wang[1,2,*] , Hai-Feng Lü[3] and Wim Ubachs[2,*]

[1] School of Electronic Information and Communications, Huazhong University of Science and Technology, Wuhan 430074, People's Republic of China
[2] Department of Physics and Astronomy, LaserLaB, Vrije Universiteit, De Boelelaan 1081 HV Amsterdam, The Netherlands
[3] School of Physics, University of Electronic Science and Technology of China, Chengdu 610054, People's Republic of China
[*] Authors to whom any correspondence should be addressed.

E-mail: yuanqingwang@hust.edu.cn and w.m.g.ubachs@vu.nl

Abstract

A Grüneisen relationship is defined for gases, following the formulation of the original microscopic Grüneisen ratio $\gamma = (d \ln \omega)/(d \ln V)$ for solids. In the case of gases acoustic excitations represent the modes at frequency ω to be considered. By comparing to measured Brillouin shifts in various gases (SF_6, N_2O, and CO_2) under various conditions of pressure and temperature, a specific value of the defined ratio $\gamma_0 = 0.064 \pm 0.004$ is found to provide a universal description of the active modes in a gas. This finding of such universal gas law may find application in extrapolation of properties of ideal gases to regimes where those cannot be measured easily, like the acoustics and shocks at extremely high temperatures.

1. Introduction

In the early 20th century, Grüneisen collected and analyzed the thermodynamic properties of atomic metals such as thermal expansion coefficients, internal energy, entropy and atomic volume [1, 2]. He defined a *dimensionless* parameter, that can be written in various forms:

$$\Gamma \equiv V \left(\frac{\partial P}{\partial E} \right)_V = V \left(\frac{\partial P}{\partial T} \right)_V \Big/ \left(\frac{\partial E}{\partial T} \right)_V \tag{1}$$

with P, T, V and E the thermodynamic quantities of pressure, temperature, volume and energy. This Grüneisen parameter can be viewed as the measure of the change in pressure produced by a change in the total energy of the system under conditions of constant volume. From collecting experimental data on metals, ranging from Sodium to Bismuth, values for the dimensionless Γ parameter were found to lie in the range (1.0–2.5) [1]. This universality of a metallic property is used in condensed matter studies [3], as a measure or constraint in phase transitions and shock waves [4], as well as in geophysics [5, 6], where the properties of the Earth's interior can only be deduced from seismological data provided that Γ is understood [7].

Attempts have been made to define a Grüneisen parameter for the gaseous phase [8]. For the case of ideal gases, with $P = nRT/V$ and $E = (3/2)nRT$ (R the ideal gas constant) this leads to the trivial result that $\Gamma = 2/3$. This relation holds for gases consisting of monatomic species. For molecules with internal degrees of freedom, these should be taken into account, leading to Grüneisen parameters of $\Gamma = 2/5$ for diatomic molecules and smaller ones for polyatomic molecules.

However, this approach ignores the view on the Grüneisen relation, connecting it to vibrational modes in a medium, following the recognition that only specific quantized modes are permitted in a solid, as in the quantum-based analyses of the specific heat of solids [9, 10]. Already by Grüneisen himself it was shown,

that a Grüneisen parameter can be defined in microscopic form:

$$\gamma \equiv -\frac{\partial \ln \omega_i}{\partial \ln V}, \tag{2}$$

where ω_i represent the vibrational modes in a material. In fact this definition is typically used as a Grüneisen scaling parameter for the treatment of solids [11] and liquids [12, 13]. It is the rationale of the present study that this microscopic definition of the Grüneisen parameter can also be used in the treatment of gases. In a gas thermal fluctuations occur that become manifest as collective effects in the form of acoustic waves. Such acoustic excitations in a medium, propagating with the speed of sound v_s, are typically observed in light scattering, where at adjacent sides of a central Rayleigh elastic peak two inelastic resonances are produced by scattering off the acoustic modes. This phenomenon of Brillouin side peaks [14] has been widely investigated, in particular since the invention of the laser via spontaneous [15] and coherent light scattering [16–19].

Typically, under different thermodynamic conditions, the Brillouin side peaks exhibit different shifts affecting the composite RB-spectral lineshape. The overall behaviour of RB-spectra can be cast into a generalised description to depend on the uniformity parameter y, which is defined as the ratio of the wavelength of incident light λ_i to the mean free path l between collisions [20, 21]. When $y \gg 1$, such as for dense media, the light scattering process is in the hydrodynamic regime and the acoustic modes will become pronounced as side peaks in the spectral profiles [22]. In the opposite case, the Knudsen regime with $y \ll 1$, the Rayleigh peak and the Brillouin peaks in the RBS spectrum are completely overlapped and the Brillouin side peaks cannot be discriminated. For the intermediary or kinetic regime, $y = \mathcal{O}(1)$, the overlapping area between the Rayleigh and Brillouin side peaks becomes less [23].

Studies on the Rayleigh–Brillouin (RB) spectral line shapes reveal thermodynamic properties of gases such as the elusive bulk viscosity [24], while there is the application of remote measurement of atmospheric temperature via RB-lidar [25]. Detailed models, based on thermodynamics, have been developed for RB-scattering spectra in the hydrodynamic regime [22], in the kinetic regime of lower pressures, e.g. the Tenti model [26], and for gases composed of binary constituents [27, 28]. Also molecular dynamics simulations have been explored to compute the RB-line shape [29, 30].
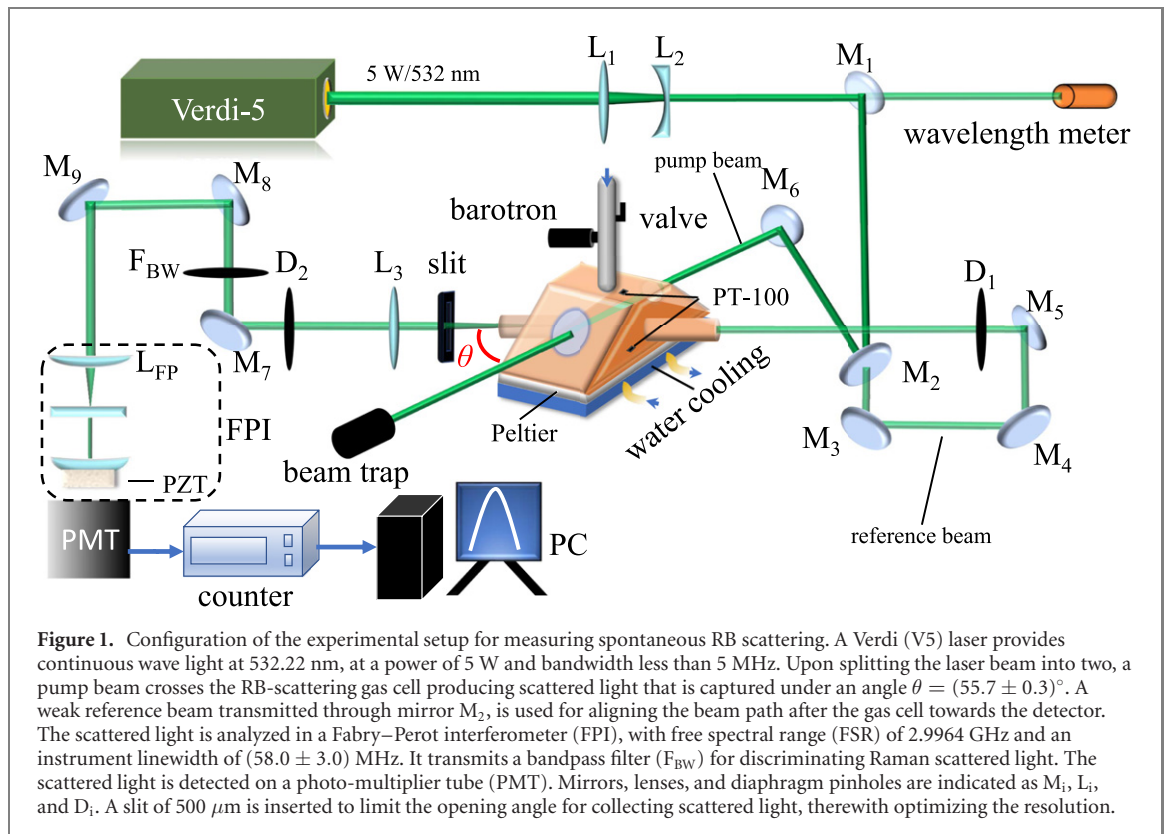
In the present paper we focus on the frequency shift of the Brillouin modes, in order to deduce a universal scaling analogous to the Grüneisen approach in solids, now with the acoustic mode taking the place of lattice vibrations to define a non-trivial Grüneisen ratio. A choice was made to investigate light scattering in sulphur hexafluoride (SF_6), nitrous oxide (N_2O), and carbon dioxide (CO_2) in view of their large Raleigh scattering cross sections. Brillouin shifts are experimentally determined for these gases in a range of pressures and temperatures, with the goal of combining resulting data in a comprehensive Grüneisen approach, which will be introduced in this work.

2. Experiment

2.1. Experimental setup

A setup for measuring spontaneous RB light scattering is used with a continuous-wave laser at a wavelength of 532.22 nm, power of 5 W, and bandwidth less than 5 MHz. The setup is sketched in figure 1. The laser light travels through a gas cell and the scattered light is collected at an angle of $\theta = 55.7 \pm 0.3°$. The choice for an angle closer to forward scattering than the usual choice of perpendicular scattering ($\theta = 90°$) provides conditions where the Brillouin side peaks are more pronounced. A similar reasoning holds for the use of green light (532 nm) resulting in more pronounced side peaks than for blue or ultraviolet light [23]. The gas scattering cell, equipped with Brewster windows, can be operated at elevated pressures up to 8 bar and a temperature control system is used to keep it at a constant temperature with uncertainty less than 0.1°C. The RB-scattered light, collected under the fixed scattering angle, is constrained by a slit for a narrow opening angle of 0.5° to accurately define the scattering geometry. The beam of scattered light further propagates through a bandpass filter (Materion, $T > 90\%$ at $\lambda_i = 532$ nm, bandwidth $\Delta\lambda = 2.0$ nm) thereby rejecting Raman-scattered light. A Fabry–Perot interferometer (FPI), equipped with a voltage-controllable piezo transducer for varying its cavity length, is used for analyzing the spectral profile of the scattered light. The FPI was calibrated by scanning an auxiliary tunable laser (a narrowband ring dye laser) over a thousand cavity modes, yielding an accurate value for the free spectral range (FSR) of 2.9964(5) GHz. The instrument width of the FPI FWHM, yielding $\sigma = 58.0 \pm 3.0$ MHz, was measured by transmitting a reference laser beam (at the fixed wavelength of 532 nm) and by scanning the piezo to determine the spectral profile of a cavity mode. The scattered photons after the FPI are detected by a PMT and stored in a computer.

The RB-spectral profile is measured by scanning the high-resolution Fabry–Perot analyzer at integration times of 1s for each step. A full spectrum covering a large number of consecutive RBS-peaks and 10 000 data

Figure 1. Configuration of the experimental setup for measuring spontaneous RB scattering. A Verdi (V5) laser provides continuous wave light at 532.22 nm, at a power of 5 W and bandwidth less than 5 MHz. Upon splitting the laser beam into two, a pump beam crosses the RB-scattering gas cell producing scattered light that is captured under an angle $\theta = (55.7 \pm 0.3)°$. A weak reference beam transmitted through mirror M_2, is used for aligning the beam path after the gas cell towards the detector. The scattered light is analyzed in a Fabry–Perot interferometer (FPI), with free spectral range (FSR) of 2.9964 GHz and an instrument linewidth of (58.0 ± 3.0) MHz. It transmits a bandpass filter (F_{BW}) for discriminating Raman scattered light. The scattered light is detected on a photo-multiplier tube (PMT). Mirrors, lenses, and diaphragm pinholes are indicated as M_i, L_i, and D_i. A slit of 500 μm is inserted to limit the opening angle for collecting scattered light, therewith optimizing the resolution.

points were obtained in about 3 h. For the methods of data collection and for a more detailed description of the experimental setup we refer to Gu *et al* [31].

2.2. Experimental results

RB-spectral data are collected for hexafluoride (SF_6) molecular gas for the pressure regime 0.5–5 bar, in which the temperature is controlled at 293.0 K ($y = [1.86, 18.41]$) and results are plotted in figure 2(a). Similarly data were collected for nitrous oxide (N_2O) molecular gas in a pressure range of $P = 1$–8 bar ($y = [1.95, 14.96]$), with results presented in figure 3(a). For the carbon dioxide (CO_2) molecular gas RB-spectral data for pressures in the range of $P = 1$–4 bar and four different temperatures ($T = 353$ K, 332 K, 313 K, and 293 K) were recorded previously [32], and are here displayed in figure 4(a). In the case of CO_2 the pressures and temperatures covered correspond to an interval for the uniformity parameter of $y = [1.91, 7.55]$.

Experimental values for the measured Brillouin shift, through peak reading of the sidebands of the RB-spectral data, are plotted as a function of pressure in figures 2(b)–4(b). It is evident that the observed Brillouin shifts f_B decrease rapidly towards low pressures, while f_B approaches to a constant in the high pressure limit. Such behaviour is itself not new, and was observed for the specific example of coherent RB-scattering in air [18].

For solids, the acoustic wavelength is generally much larger than the crystal lattice constant, hence the atomic discontinuity can be ignored. This also holds for liquids. Debye's phonon theory [10] describes the vibrational modes, with elastic standing waves in the crystal lattice being independent and the interaction between corresponding phonons negligible. The elasticity results in a harmonic approximation. The values of the Brillouin shift can be derived in terms of angular frequency (ω_B^h) or frequency (f_B^h) [23, 33]:

$$f_B^h = \frac{\omega_B^h}{2\pi} = \frac{2n_i v_s}{\lambda_i} \sin\left(\frac{\theta}{2}\right), \tag{3}$$

where λ_i is the wavelength of the light, θ the scattering angle, n_i the refractive index, and v_s the sound speed with [33]:

$$v_s = \sqrt{c_p k_B T / c_v m}, \tag{4}$$

with m the molecular mass, c_p and c_v the specific heats, and k_B the Boltzmann constant. Here $c_v = c_{trans} + c_i$, with the translational heat capacity c_{trans} equalling $3R/2$ (for three translational degrees of freedom). For the internal heat capacity c_i we adopt a result obtained in previous studies on the modeling of RB-scattering, where it was shown that the vibrational relaxation is frozen under the high-frequency
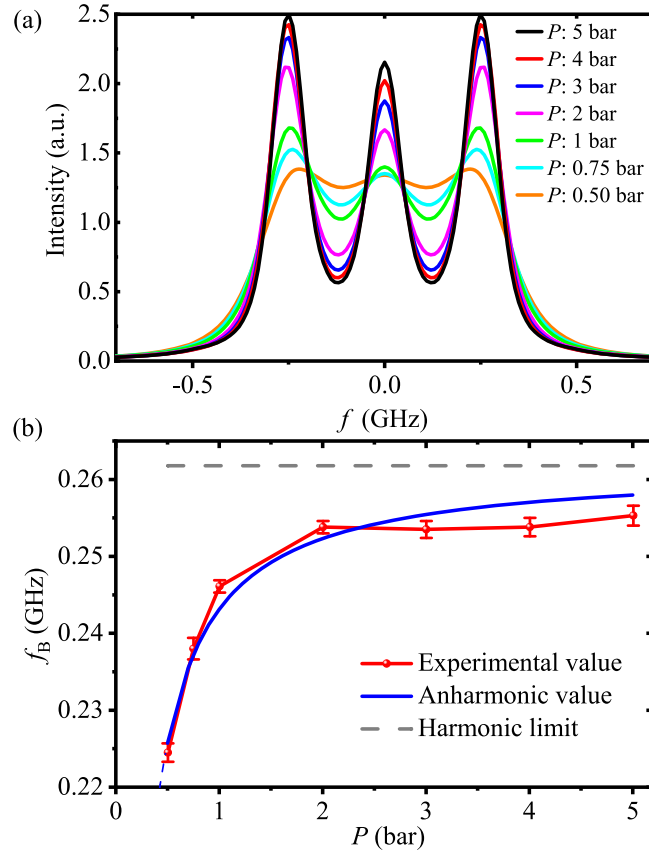
Figure 2. (a) Experimental RB-spectral profiles of SF_6 measured at $\lambda = 532.22$ nm, a scattering angle of 55.7°, temperature of 293.0 K, for various pressures P; the integrated intensity is normalized. (b) Extracted Brillouin shifts from experimental data (red), and computed values from equation (7) (blue); the (grey) dashed line represents the harmonic limit corresponding to equation (3).

conditions of Brillouin scattering. This was discussed in results for SF_6 [34], N_2O [35] and CO_2 [32]. Hence, only rotational degrees of freedom are considered, and for SF_6 $c_i = 3R/2$ is taken, and $c_i = R$ for N_2O and CO_2. Hence, the specific heat ratio c_p/c_v is taken as $4/3$ for SF_6, and $7/5$ for N_2O and CO_2 in the evaluation of the Brillouin shift.

By evaluating equations (3) and (4) the values for the Brillouin shift f_B can be computed and be found independent of pressure. Results are displayed in figures 2(b)–4(b), where in the last case of CO_2 the computation is performed for various temperatures. The experimental values for the Brillouin shift for the highest pressures approach the thus computed values for f_B. Indeed, this is congruent with the fact that at high pressures the distance between gas molecules decreases and enters the hydrodynamic regime, where the discontinuity between the gas molecules becomes negligible and the gas can be considered as an elastic medium. With the decrease of pressure, f_B decreases and deviates gradually from the values of this model, based on elastic waves and an harmonic approximation. Hence we conclude, that results from this harmonic approximation are not in agreement with experimental findings.

3. Microscopic Grüneisen parameter for gases

For an analysis of the differences between the calculated harmonic values and experimental values, the microscopic definition of the Grüneisen parameter will be used for the treatment of gases.

In gases, the sound wavelength becomes comparable to the molecular mean free path [36], in particular at low pressures [37]. Hence, the molecular discontinuity and the interaction between phonons cannot be ignored. This theory, that goes beyond Debye's phonon theory of elastic waves, will be referred to as anharmonic.

To take the anharmonic effect into account, we resort to the microscopic formulation of the Grüneisen relationship, as in equation (2), describing the dependence of the phonon frequency ω on the molar volume of the medium V [38]. The negative sign indicates that as molar volume V increases, the phonon frequency decreases. If the Grüneisen parameter γ is considered as a constant and independent of pressure, based on
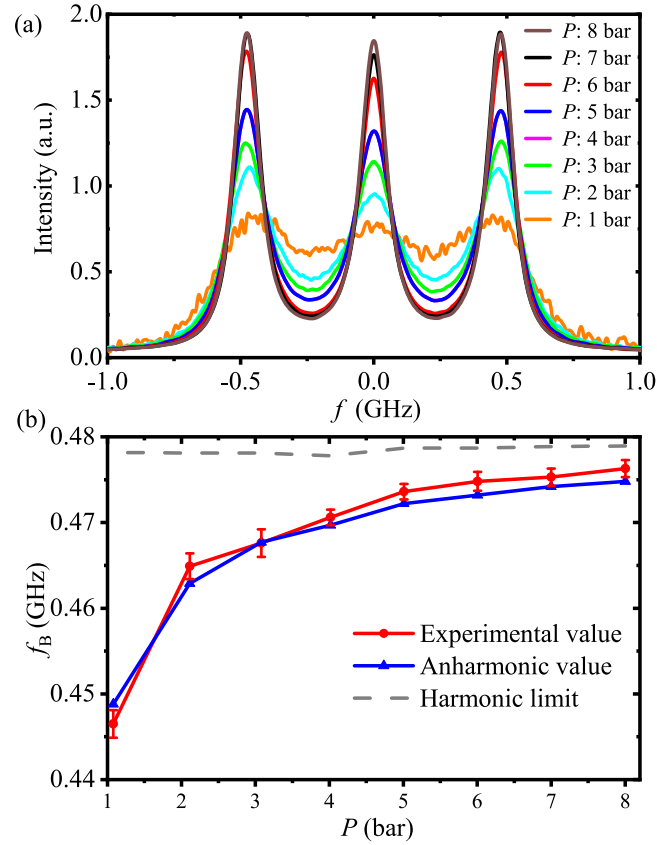
Figure 3. (a) RB-spectra for N_2O gas, under different pressure conditions at $T \approx 295$ K. These data were measured at an incident wavelength of $\lambda = 532.22$ nm and $\theta = 55.7°$. (b) Extracted Brillouin shifts from experimental data (red), and computed values from equation (7) (blue); the (grey) dashed line represents the harmonic limit corresponding to equation (3); note that the line is not straight because the data at various pressures were obtained at slightly differing temperatures.

equation (2), the anharmonic Brillouin angular frequency shift can be deduced by integration:

$$\omega = \omega_0(V/V_0)^{-\gamma}. \tag{5}$$

For high pressures the phonon angular frequency approaches the limit of ω_B and the harmonic approximation prevails, as in solids and liquids. Hence, for the scaling constant ω_0 we adopt ω_B^h and we will refer to it as the harmonic limit. The molar volume V_0 is taken at the reference temperature of $T_0 = 273$ K and reference pressure of $P_0 = 1$ bar. When fitting the experimental data with the predicted values from equation (5), a large deviation results by adopting a pressure-independent γ. Therefore, the assumption of γ as a constant value for gases does not hold, although it is generally adopted in condensed matter physics.

It had indeed been pointed out that for low density matter, the Grüneisen parameter should not be taken as a constant [39, 40], but rather in a linear relationship as $\gamma(V) = \gamma_0 V/V_0$, with molar volume V, and γ_0 a reference Grüneisen parameter under reference density n_0, and reference molar volume V_0. The phonon angular frequency can then be obtained for the anharmonic case as:

$$\omega_B^{ah} = \omega_0 \, e^{-\gamma_0 V/V_0}. \tag{6}$$

Compared with equation (5), the dependence of the Brillouin shift on the system molar volume turns into an exponential relationship rather than a power-law relationship. Again, we can equate the integration constant ω_0 to ω_B^h as occurring in the harmonic limit.

The analysis based on the microscopic Grüneisen parameter yields an expression for the Brillouin shift that scales with molar volume or equivalently, the pressure via equation (6). In this way the microscopic Grüneisen parameter enters the expression for the Brillouin shift. By rewriting the volume V via the ideal gas law $PV = nRT$ (R the universal gas constant) the derivation finally yields:

$$f_B^{ah} = \frac{2n_i}{\lambda_i} v_s \, e^{-\gamma_0 \frac{RT}{V_0 P}} \, \sin\left(\frac{\theta}{2}\right). \tag{7}$$

This result is important since it explicitly yields a pressure dependence of the Brillouin shift.
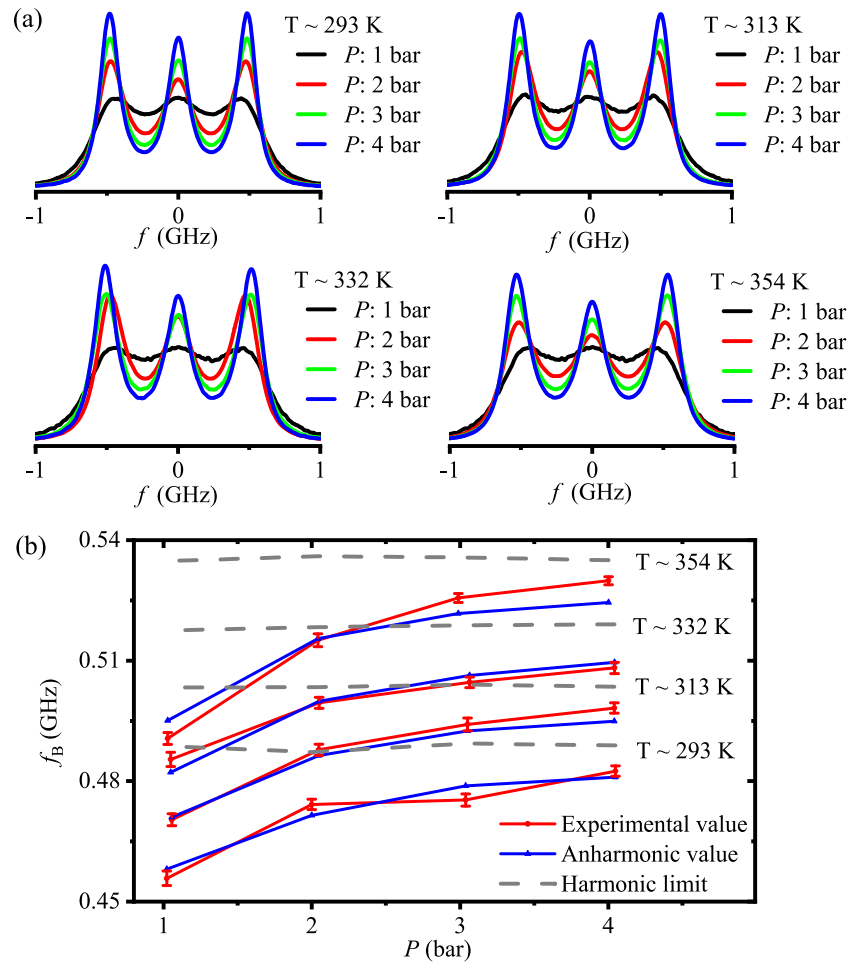
Figure 4. (a) RB-spectra of CO_2 taken under different P and T conditions, and at $\lambda = 532.22$ nm and $\theta = 55.7°$. Data reproduced from [32]. (b) Extracted Brillouin shifts from experimental data (red), and computed values from equation (7) (blue); the (grey) dashed lines represent the harmonic limits corresponding to equation (3), as computed for the different temperatures.

In the first example the experimental values obtained for SF_6 gas were inserted in the equation, while a fit was made to extract the value of γ_0. The comprehensive data set for SF_6 for all pressures led to a single value of $\gamma_0 = 0.068$. In this approach the experimental data for the Brillouin shift could be reproduced within a relative error in γ_0 as small as $0.8\%-1.3\%$ for the wide range of pressures studied experimentally. This is graphically shown in figure 2(b). The blue curve representing the thus obtained anharmonic values agree very well with the experimental data for the Brillouin shifts, represented by the red points.

As for the second example Brillouin shifts were measured for N_2O molecular gas at $\lambda_i = 532.22$ nm and $\theta = 55.7°$. Experimental results compared with the anharmonic approach are presented in figure 3(b). Again very good agreement is found with the measured values for the Brillouin shift for a microscopic Grüneisen parameter, in this case for a fitted value of $\gamma_0 = 0.063$.

In the third example the experimental RB-spectral data for CO_2, as previously reported [32], were reanalyzed in the framework of the present Grüneisen approach. The Brillouin shifts obtained from the experiments agree well with the prediction from equation (7), where now a value of $\gamma_0 = 0.060$ is fitted. For these data of CO_2 a harmonic limit is computed for each temperature in view of the fact that f_B depends on temperature via the velocity of sound, cf equation (4). This gives rise to a scaling of the harmonic limit with $\sqrt{T}$, quantitatively in agreement with the high-pressure asymptotic values as obtained in experiment. For RB-shifts at lower pressures an additional exponentially decaying temperature dependence comes into play, which is explicit in equation (7). Hence in this example of the CO_2-data the approach of the microscopic Grüneisen relation is extended to varying temperatures.

The consistency of the presented experimental results with a microscopic Grüneisen model for ideal gases is shown to be valid for gases of various nature, various spherical and linear geometries, various masses, various degrees of freedom, various specific heat ratios c_p/c_v, and measured under different conditions of gas pressure and temperature. In all cases the model predicts and quantitatively explains a
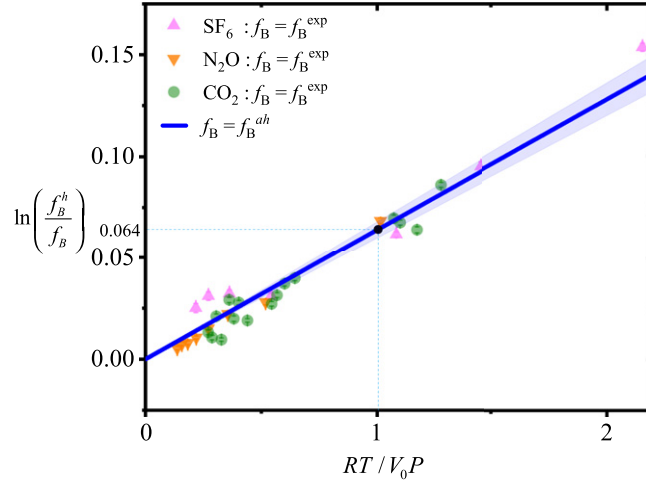
Figure 5. Universal behaviour of the Brillouin shift in gases, captured by a single parameter γ_0. Individual data points relate to the experimentally determined Brillouin shifts for the three gases (at various pressures and temperatures), indicated with symbols specified in the legend, and scaled to the value of the harmonic limit f_B. The full line represents the slope computed from equation (8) for the fitted values of $\gamma_0 = 0.064$.

drop in the Brillouin shift toward lower pressures, by invoking only a single scaling parameter which adopts a single universal value for all examples analyzed. When averaged over all comprehensive data we find $\gamma_0 = 0.064 \pm 0.004$.

To further demonstrate this apparent universal scaling of the Brillouin shift we combine the equations for the Brillouin shift in the harmonic limit f_B^h with the predicted shift in the anharmonic case as used in the microscopic Grüneisen approach, f_B^{ah}, to yield:

$$\ln\left(\frac{f_B^h}{f_B^{ah}}\right) = \gamma_0 \frac{RT}{V_0 P}. \tag{8}$$

In figure 5 this universal relationship is plotted for all data on all three molecules analyzed here. The full line represents the theoretical curve for $\ln(f_B^h/f_B)$ as a function of (RT/V_0P), averaged over all data with $\gamma_0 = 0.064$, while the singular data entries represent the values of experimental shifts scaled to the harmonic limit f_B^h. The slope represents the dimensionless Grüneisen parameter γ_0, which is in case of the data for CO_2 modified for the temperature appearing in the exponent of equation (7). As $1/P$ approaches zero, hence at the origin, the Brillouin shift equals the value f_B, i.e. the harmonic limit.

The graphical representation of all collapsed data in figure 5 provides proof that γ_0 is an effective dimensionless parameter in the realm of gases, analogous to the microscopic Grüneisen parameter defined for solids in the early 20th century. With the increase of $1/P$, the anharmonic effect generates a considerable deviation of the Brillouin shift from the value f_B, which is a value that can be obtained from a model involving harmonic oscillations induced by temporal fluctuations, here treated as a harmonic limit. As illustrated in figures 2–4, the experimental data in the kinetic and hydrodynamic regimes are well fitted by equation (7). The here derived microscopic Grüneisen relationship and the universal parameter is expected to be applicable to a wider range of pressure conditions, especially at lower pressures when a traversal is made from the kinetic regime to the Knudsen regime. As is known from RB-scattering studies at low pressures, e.g. for sub-atmospheric pressures prevailing in the upper layers in the Earth's atmosphere [23], the Brillouin shifts at adjacent sides of the central Rayleigh peak can no longer be distinguished. With the knowledge of the Grüneisen parameter γ_0, extrapolations can be made on the collective properties in such dilute gaseous media.

4. Conclusion

In summary, a Grüneisen relationship was derived for ideal gases, that goes beyond a trivial approach discarding acoustics and that had led to a Grüneisen ratio of 2/3. The approach chosen was based in analogy to the formulation of the original microscopic Grüneisen ratio [1, 2] for solids. Key feature is that thermal fluctuations and resulting acoustic modes take the place of lattice vibrations, but their motion is shown to be anharmonic. By comparing to measured Brillouin shifts in various gases (SF_6, N_2O, and CO_2), a specific value of the defined ratio $\gamma_0 = 0.064 \pm 0.004$ turned out to provide a universal description of the acoustics

in a gas, represented by the Brillouin shift. It is noted that the actual value found for γ_0 is somewhat arbitrary, since it depends on the specific choice of reference parameters, the gaseous properties n_0, P_0, V_0 and T_0. This finding of a universal gas law may find application in extrapolation of properties of ideal gases to regimes where those cannot be measured easily, like the acoustics and shocks at extremely high temperatures, or the study of collective effects at low pressures.

Acknowledgments

Data availability statement

The data that support the findings of this study are available upon reasonable request from the authors.

ORCID iDs

Kun Liang ⓘ https://orcid.org/0000-0003-3954-8340
Yuanqing Wang ⓘ https://orcid.org/0000-0003-4895-5271
Wim Ubachs ⓘ https://orcid.org/0000-0001-7840-3756

References

[1] Grüneisen E 1908 Zusammenhang zwischen Kompressibilität, thermischer Ausdehnung, Atomvolumen und Atomwärme der Metalle *Ann. Phys.* **331** 393–402
[2] Grüneisen E 1912 Theorie des festen Zustandes einatomiger Elemente *Ann. Phys.* **344** 257–306
[3] Zhu L, Garst M, Rosch A and Si Q 2003 Universally diverging Grüneisen parameter and the magnetocaloric effect close to quantum critical points *Phys. Rev. Lett.* **91** 066404
[4] Brown J M and McQueen R G 1986 Phase transitions, Grüneisen parameter, and elasticity for shocked iron between 77 GPa and 400 GPa *J. Geophys. Res.* **91** 7485–94
[5] Boehler R 1993 Temperatures in the Earth's core from melting-point measurements of iron at high static pressures *Nature* **363** 534–6
[6] Stacey F D and Hodgkinson J H 2019 Thermodynamics with the Grüneisen parameter: fundamentals and applications to high pressure physics and geophysics *Phys. Earth Planet. In.* **286** 42–68
[7] Anderson O L 2000 The Gruneisen ratio for the last 30 years *Geophys. J. Int.* **143** 279–94
[8] de Souza M, Menegasso P, Paupitz R, Seridonio A and Lagos R E 2016 Grüneisen parameter for gases and superfluid helium *Eur. J. Phys.* **37** 055105
[9] Einstein A 1907 Die Plancksche Theorie der Strahlung und die Theorie der spezifischen Wärme *Ann. Phys.* **327** 180–90
[10] Debye P 1912 Zur Theorie der spezifischen Wärmen *Ann. Phys.* **344** 789–839
[11] Chandra S 2021 A comparative study of second and third order Grüneisen parameter for solids *Comput. Condens. Matter* **27** e00556
[12] Knopoff L and Shapiro J N 1970 Pseudo-Grüneisen parameter for liquids *Phys. Rev. B* **1** 3893
[13] Mausbach P, Köster A, Rutkai G, Thol M and Vrabec J 2016 Comparative study of the Grüneisen parameter for 28 pure fluids *J. Chem. Phys.* **144** 244505
[14] Brillouin L 1922 Diffusion de la lumière et des rayons X par un corps transparent homogène *Ann. Phys.* **9** 88
[15] Greytak T J and Benedek G B 1966 Spectrum of light scattered from thermal fluctuations in gases *Phys. Rev. Lett.* **17** 179
[16] Pan X, Shneider M N and Miles R B 2002 Coherent Rayleigh–Brillouin scattering *Phys. Rev. Lett.* **89** 183001
[17] Vieitez M O, van Duijn E J, Ubachs W, Witschas B, Meijer A, de Wijn A S, Dam N J and van de Water W 2010 Coherent and spontaneous Rayleigh–Brillouin scattering in atomic and molecular gases, and gas mixtures *Phys. Rev. A* **82** 043836
[18] Gerakis A, Shneider M N and Barker P F 2011 Coherent Brillouin scattering *Opt. Express* **19** 24046–54
[19] Cornella B M, Gimelshein S F, Shneider M N, Lilly T C and Ketsdever A D 2012 Experimental and numerical analysis of narrowband coherent Rayleigh–Brillouin scattering in atomic and molecular species *Opt. Express* **20** 12975–86
[20] Cercignani C 1969 *Mathematical Methods in Kinetic Theory* (Berlin: Springer)
[21] Miles R B, Lempert W R and Forkey J N 2001 Laser Rayleigh scattering *Meas. Sci. Technol.* **12** R33
[22] Letamendia L, Chabrat J P, Nouchi G, Rouch J, Vaucamps C and Chen S 1981 Light-scattering studies of moderately dense gas mixtures: hydrodynamic regime *Phys. Rev. A* **24** 1574
[23] Wang Y, Gu Z, Liang K and Ubachs W 2021 Rayleigh–Brillouin light scattering spectroscopy of air; experiment, predictive model and dimensionless scaling *Mol. Phys.* **119** e1804635
[24] Gu Z and Ubachs W 2013 Temperature-dependent bulk viscosity of nitrogen gas determined from spontaneous Rayleigh–Brillouin scattering *Opt. Lett.* **38** 1110
[25] Witschas B, Gu Z Y and Ubachs W 2014 Temperature retrieval from Rayleigh–Brillouin scattering profiles measured in air *Opt. Express* **22** 29655–67

[26] Boley C D, Desai R C and Tenti G 1972 Kinetic models and Brillouin scattering in a molecular gas *Can. J. Phys.* **50** 2158

[27] Gu Z, Ubachs W, Marques W and van de Water W 2015 Rayleigh–Brillouin scattering in binary-gas mixtures *Phys. Rev. Lett.* **114** 243902

[28] Wang Y, Ubachs W, de Moraes C A M and Marques W 2021 Rayleigh–Brillouin scattering in binary mixtures of disparate-mass constituents: SF_6-He, SF_6-D_2, and SF_6-H_2 *Phys. Rev. E* **103** 013102

[29] Jamali S H, de Groen M, Moultos O A, Hartkamp R, Vlugt T J H, Ubachs W and van de Water W 2019 Rayleigh–Brillouin light scattering spectra of CO_2 from molecular dynamics *J. Chem. Phys.* **151** 064201

[30] Ma Q, Yang C, Bruno D and Zhang J 2021 Molecular simulation of Rayleigh–Brillouin scattering in binary gas mixtures and extraction of the rotational relaxation numbers *Phys. Rev. E* **104** 035109

[31] Gu Z, Vieitez M O, van Duijn E J and Ubachs W 2012 A Rayleigh–Brillouin scattering spectrometer for ultraviolet wavelengths *Rev. Sci. Instrum.* **83** 053112

[32] Wang Y, Ubachs W and van de Water W 2019 Bulk viscosity of CO_2 from Rayleigh–Brillouin light scattering spectroscopy at 532 nm *J. Chem. Phys.* **150** 154502

[33] Fabelinskii I L 1968 *Some Theoretical Studies of the Spectral Composition of Molecularly Scattered Light Molecular Scattering of Light* (Berlin: Springer) pp 81–154

[34] Wang Y, Yu Y, Liang K, Marques W, van de Water W and Ubachs W 2017 Rayleigh–Brillouin scattering in SF_6 in the kinetic regime *Chem. Phys. Lett.* **669** 137–42

[35] Wang Y, Liang K, van de Water W, Marques W and Ubachs W 2018 Rayleigh–Brillouin light scattering spectroscopy of nitrous oxide (N_2O) *J. Quant. Spectrosc. Radiat. Transf.* **206** 6369

[36] Yano T 2012 Molecular simulation of sound for development of nanoacoustics *Acoustics 2012* (Nantes, France April 2012) https://hal.archives-ouvertes.fr/hal-00811370/

[37] Maksymov I S and Greentree A D 2019 Coupling light and sound: giant nonlinearities from oscillating bubbles and droplets *Nanophotonics* **8** 367–90

[38] Roufosse M C and Jeanloz R 1983 Thermal conductivity of minerals at high pressure: the effect of phase transitions *J. Geophys. Res.* **88** 7399–409

[39] Greeff C W and Graf M J 2004 Lattice dynamics and the high-pressure equation of state of Au *Phys. Rev. B* **69** 054107

[40] Reynolds C L Jr and Couchman P R 1976 Volume dependence of phonon frequencies *J. Appl. Phys.* **47** 2779